LES of the flow around two cylinders in tandem

G. Palau-Salvador[a],*, T. Stoesser[b], W. Rodi[c]

[a]*Rural Engineering Department, Polytechnical University of Valencia, camino de vera s/n, 46022 Valencia, Spain*
[b]*School of Civil and Environmental Engineering, Georgia Institute of Technology, 790 Atlantic Drive, 30322 Atlanta, USA*
[c]*Institute for Hydromechanics, Karlsruhe University, Kaiserstrasse 12, 76128 Karlsruhe, Germany*

Abstract

The flow around an arrangement of two cylinders in tandem exhibits a remarkably complex behaviour that is of interest for many engineering problems, such as environmental flows or structural design. In the present paper, a Large Eddy Simulation using a staggered Cartesian grid has been performed for the flow around two cylinders in tandem of diameter $D = 20$ mm and height $H = 50$ mm submerged in an open channel with height $h = 60$ mm. The two axes have a streamwise spacing of $2D$. The Reynolds number is 1500, based on the cylinder diameter and the free-stream velocity u_∞. The results obtained show that no vortex shedding occurs in the gap between the two cylinders where the separated shear layers produced by the upstream cylinder reattach on the surface of the downstream one. The flow separates on the top of the first cylinder with the presence of two spiral nodes known as owl-face configuration. On top of the downstream cylinder, the flow is attached. A complex mean flow develops in the gap and also behind the second cylinder. Comparisons with PIV measurements reveal good general agreement, but there are differences concerning some details of the flow in the gap between the cylinders.

1. Introduction

The flow around two cylinders (either of finite of infinite height) in tandem represents an important and remarkably complex flow configuration that has been the subject of experimental and numerical investigations for several decades [e.g., Igarashi (1981), Zdravkovich (1987)]. This configuration has an important relevance for the study of flows around buildings (Luo et al., 1987), forces on bridge piers (Kadota et al., 2007) or turbulence in vegetated open channels (Fischer-Antze et al., 2001).

The interference that arises when more than one body is placed within the fluid stream is responsible for several changes in the characteristics of the flow. Depending on the distance between the cylinders, different flow regimes can occur and in the case of finite height cylinders mainly two-dimensional large-scale structures are present. Classifications of qualitative flow regimes of the tandem cylinder arrangement can be found in Igarashi (1981) and Zdravkovich (1987). Essentially, there is a critical value of L/D (L being the distance between the axes of the cylinders and D the diameter of each cylinder) below which no vortex shedding occurs in the gap region. At this value, the flow changes from a co-shedding type, with both cylinders shedding vortices, to the reattached type. The latter is characterized by a shear layer that separates from the upstream cylinder and reattaches on the downstream cylinder (Zdravkovich, 1987).

According to the latter description, one can classify the flow around two-in-tandem cylinders in four types: *single-slender-body regime*, due to the proximity of the cylinders, the shear layer from the upstream cylinder rolls up after the downstream cylinder, forming a single wake; *quasi-steady reattachment regime*, the shear layer of the upstream cylinder reattaches on the downstream one; *unstable region*, vortex shedding behind the front cylinder occurs, but is intermittently suppressed and replaced by the reattachment flow regime; and the *co-shedding region*, where vortex shedding occurs past both cylinders. The critical value and the appearance of each flow regime depend on the Reynolds number as the experiments by Zdravkovich (1987) and Ljungkrona et al. (1991) have shown.

When the cylinders are of finite height, additional trailing vortices originating at the free end of the cylinders come into play adding further complexity to the flow. The tandem arrangement can be viewed as a simplification of an array of a large number of cylinders, and some of the characteristics of the tandem flow should be present, at least to some degree, also in an array.

Several qualitative flow-visualizations of the gap and near-wake flow patterns are reported in the literature. Oka et al. (1972) measured vortex-shedding frequencies; they did not observe any shedding until a gap distance greater than 3.8 diameters. Other authors found similar values: Tanida et al. (1973) obtained a value of 3 diameters and Igarashi (1981) of 3.53 diameters. However, other authors, like Ljungkrona et al. (1991) clearly show the important influence of the Reynolds number on the critical value of L/D (4.5 for Re = 1400 and 3.0 for Re = 42 000). Summer et al. (1999) and Kadota et al. (2007) used Particle Imaging Velocimeter to measure the flow in the gap region of the two cylinders in tandem.

Apart from the above experimental studies, very few numerical simulations exist which furthermore are mostly two-dimensional, investigating infinite-height cylinders. Simulation of the vortex patterns and steady as well as unsteady loading at low Reynolds numbers was undertaken by Stansby et al. (1987) using a vortex method. Recent efforts, employing different types of numerical simulation, include those of Mittal et al. (1997) and Farrant et al. (2000), also at relatively low values of Reynolds number. Furthermore, Papaioannou et al. (2006) studied the three-dimensional effects in flow around two stationary cylinders with laminar and early turbulent regimes using a spectral/hp element method.

This paper presents results of Large Eddy Simulations (LESs) of flow in an open channel over and around two submerged cylinders, one located downstream of the other. A high resolution grid is employed in the vicinity of the cylinders to obtain precise information on the zone around and between the cylinders. To the best of our knowledge, this is the first investigation of such a flow with the two finite-height cylinders arranged in tandem.

2. Configuration investigated

The flow around two cylinders of finite height arranged in tandem, where one cylinder is located downstream of the other, studied here corresponds to an experiment carried out by Kadota et al. (2007). These authors performed measurements on various configurations of submerged two-in-tandem cylinders with a two-dimensional Particle Image Velocimetry (PIV) system in a water tunnel. In their flume experiments, two cylinders of diameter $D = 20$ mm and height $H = 50$ mm were submerged under different water level heights h (in the present simulations we used $h = 60$ mm) and at a spacing L of $2D$. The Reynolds number based on the cylinder diameter and the free-stream velocity u_∞ is 1500. Prior to the simulations, the experimenters provided the information that the approach flow was almost uniform, with a very thin boundary layer. For $L/D = 2$, the flow corresponds to the *quasi-steady reattachment regime* where no vortex shedding occurs in the gap region.

The calculation domain spans 12.5D in streamwise, 6D in spanwise and 3D in vertical direction (i.e., the full water depth), respectively (Fig. 1). The width and the height of the computational domain were selected to correspond to the flow cross section in the experiment. The origin of coordinate system was placed at the base of the first cylinder and x, y, z represent the streamwise, wall-normal and lateral direction, respectively. The grid consists of $516 \times 256 \times 192$ grid points in streamwise, spanwise and vertical directions, respectively, which sums to a total of approximately 25 million grid points. The grid spacings in terms of wall units are the same in all directions, namely $\Delta_x^+ = \Delta_y^+ = \Delta_z^+ \approx 1$. Fig. 2 shows the grid in a horizontal and a vertical plane indicating the refinement of the grid towards the cylinders (note that only every 5th grid line is plotted). The outflow is located at $x/D = 9.5$ where a convective condition is applied. At the inflow ($x/D = -3.5$) a constant velocity $u = u_\infty$ without fluctuations is specified. At the channel bed and lateral walls as well as the cylinder walls, the no-slip condition is used and the free surface is set as a frictionless rigid lid, treated by the slip condition.

3. Numerical method and LES modelling

The LES code MGLET, originally developed at the Institute for Fluid Mechanics at the Technical University of Munich (Tremblay and Friedrich, 2001) was used to perform the LESs. The code solves the filtered Navier–Stokes
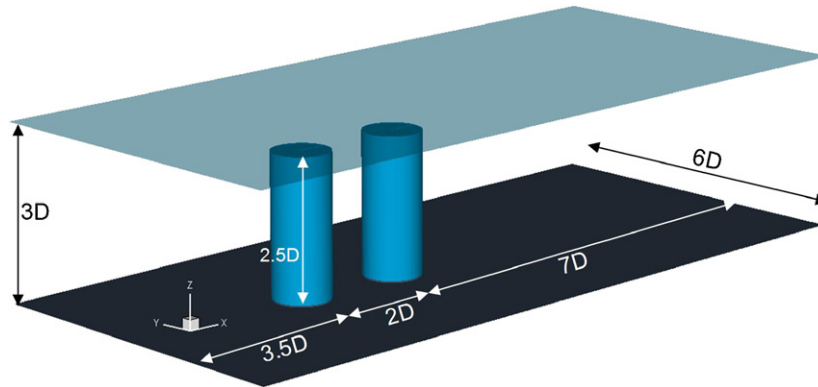
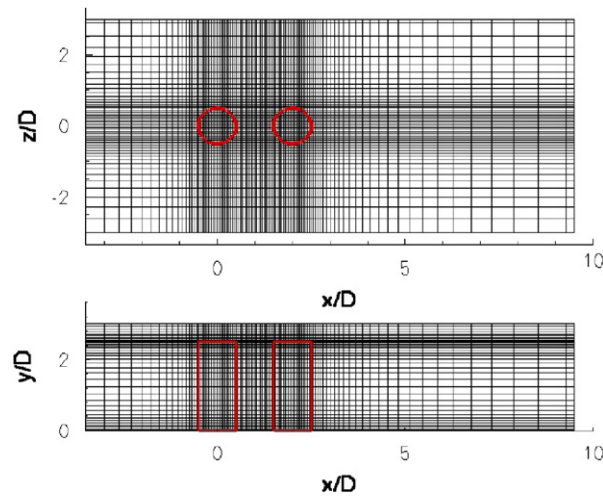Fig. 1. Schematic of the domain used in the simulation.

Fig. 2. Two-dimensional cuts in wall-parallel direction (top) and wall-normal direction (bottom) through the computational grid. Only every 5th point is plotted.

equations discretised with the finite-volume method on a staggered Cartesian grid. Convective and diffusive fluxes are approximated with central differences of second order accuracy and time advancement is achieved by a second order, explicit Adams–Bashford scheme. The Poisson equation for coupling the pressure to the velocity field is solved iteratively with the SIP method of Stone (1968). The subgrid-scale stresses appearing in the filtered Navier–Stokes equations are computed using the dynamic approach of Germano et al. (1991). The no-slip boundary condition is applied on the surface of the cylinders where the immersed boundary method is employed (Verzicco et al., 2000). This method is a combination of applying body forces in order to block the cells that are fully inside the cylinder and a Lagrangian interpolation scheme of third order accuracy, which is used for the cells that are intersected by the surfaces of the cylinders to maintain the no-slip condition.

4. Results and discussion

The results will be presented in two stages. First, the instantaneous flow will be discussed by means of the structures visualized by an iso-surface of the pressure fluctuation within the flow. Second, the average flow will be described by comparison to the experiments performed by Kadota et al. (2007).

4.1. Instantaneous flow

An impression of the complex flow structures can be obtained from Fig. 3, where a snapshot of an iso-surface of the normalized instantaneous pressure fluctuation (obtained as the difference between the instantaneous and average pressure) is plotted. The following comments are based on this picture and other views and animations not shown in the present paper. Previous (Froehlich and Rodi, 2004) and ongoing research has yielded comprehensive information about the turbulent structures that occur in the flow past single finite-height cylinders of different height-to-diameter ratios (H/D) albeit at higher Reynolds numbers (in the range 22 000–43 000). In these cases, vortex shedding occurs near the ground plate and could be observed more clearly the larger the ratio H/D is. A pair of trailing vortices originating from the top is swept downstream, reducing the vortex shedding in the upper part of the cylinder. In the present case of two-in-tandem cylinders, a different flow occurs downstream of the first cylinder. From Fig. 4 it is apparent that the shear layer separating from the cylinder side rolls up into a vortical structure (VS). However, due to the presence of the second cylinder, this disintegrates into small-scale hairpin-type vortex (HPV) structures so that no vortex street develops and there are no large-scale structures typical of shed vortices in this region. Further, the shear layers separating on both sides from the first cylinder reattach on the second cylinder. In the far field downstream of the second cylinder, larger structures are present and increase in size, but considerably less so than in the case of the single cylinder simulated by Froehlich and Rodi (2004). The animations in a plane located at mid-height of the cylinder clearly show vortex shedding in this region and allow the determination of a Strouhal number of 0.18, close to the value of 0.175 obtained experimentally by Igarashi (1981) for the same separation between cylinders but at a higher Reynolds number of 35 000. At the ground plate in front of the first cylinder a horseshoe vortex (HSV) can be seen which is thin because the boundary layer developing in the LES along the ground plate is thin at the location of the first cylinder. The view on the foot of the second cylinder is obscured, but there is probably no HSV forming there because of the complex approach flow.

4.2. Average flow

The average flow is now discussed, starting with what happens on the surface of both cylinders. Fig. 5 presents the streamlines as seen from the side and from the rear on the surfaces on both cylinders. First of all, a considerable
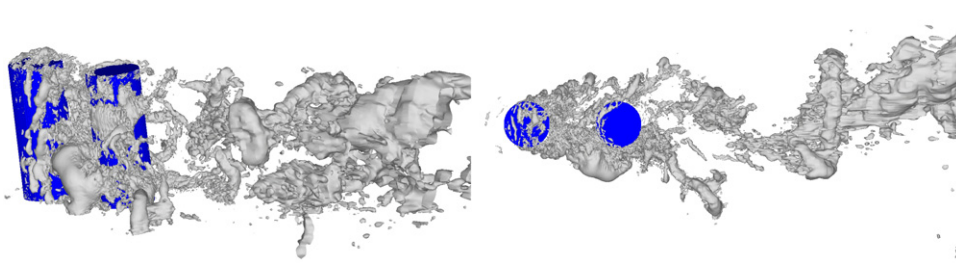

Fig. 3. Instantaneous flow structures obtained by the pressure fluctuation ($p = 0.05$) viewed from an oblique angle from the rear (left) and from the top (right).
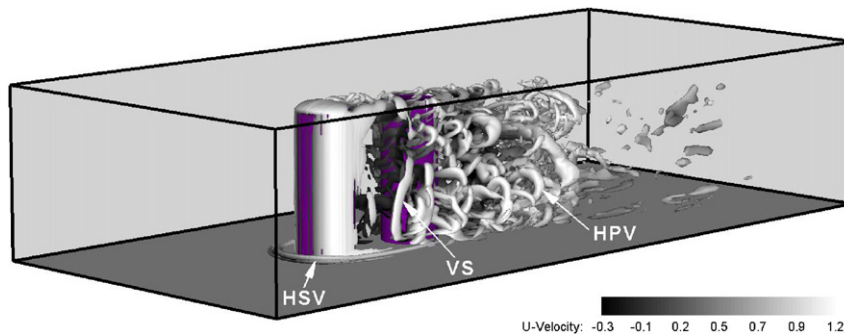

Fig. 4. Vortex structures visualized by iso-surfaces of the Q-criterion (Hunt et al., 1988).
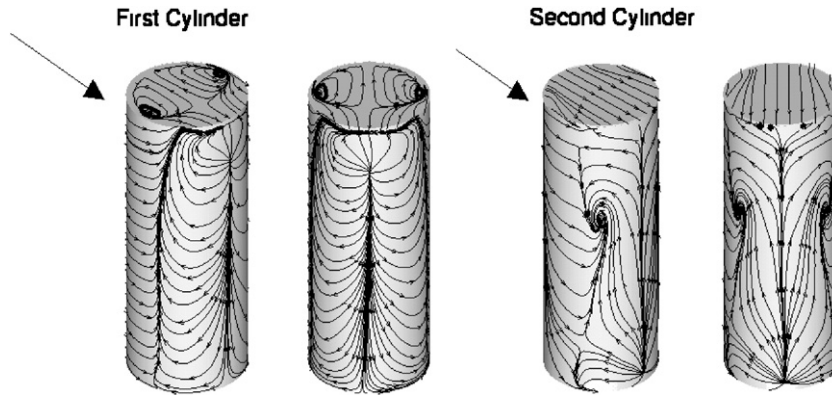
Fig. 5. Surface streamlines from both cylinders. In either case, left is the oblique view while right is the rear view.
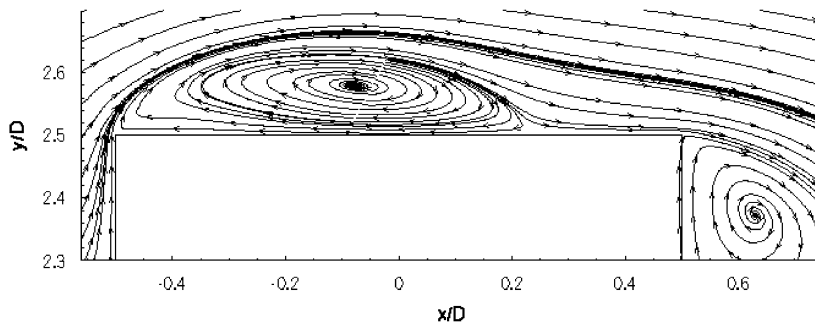

Fig. 6. Close-up of the separation over the free end of the upstream cylinder, showing a large recirculation.

difference can be seen on the free end of the cylinders. On the top of the upstream cylinder, the flow separates at the front corner and reattaches at $x/D \approx 0.2$ (see Fig. 6), leading to a recirculation and reverse flow in the front part of the top as can be observed as well in Fig. 5. This separation was not found in the experiments of Kadota et al. (2007), probably due to a lack of resolution of the PIV measurements, but it has been reported in various single finite-height cylinder measurements [e.g., Roh and Park (2003), Delery (1992), Pattenden et al. (2005), and Hain et al. (2007)]. In these also the corresponding pair of vertical vortices on the top surface was observed by oil flow pictures and smoke visualization, which represent the spiral nodes of the well-known owl-face configuration that can be seen in Fig. 5. However, on the top of the second cylinder the flow is attached because the approach flow is more or less parallel to the top plane (see Fig. 7) so that also the owl-face structure is absent and the surface streamlines are more or less parallel in the main flow direction. On the cylinder side surfaces, there is a clear nearly vertical separation line on the first cylinder, while the situation is more complex on the sides of the second cylinder. In the gap between the cylinders, the trailing vortices originating from the top of the first cylinder are moved downward and inward by the mean motion (see Fig. 7) and impinge at about half height on the second cylinder leading to a nodal point of the separation line. Also, over most of the cylinder height, the motion is downward in the rear part of the first cylinder, only near the top it is upward as the flow separates at the trailing edge and forms a small recirculation region shown in Fig. 7. In contrast, the flow in the rear of the second cylinder is directed upwards from the bottom to the very top, as is clear also from Fig. 7. Calculation of the mean drag coefficient (based on the drag force calculated by integration of the pressure over the surface, the projection area of the cylinder and the bulk velocity) for both cylinders yields values of $C_D = 1.21$ for the upstream cylinder and $C_D = 0.10$ for the downstream cylinder, which clearly underlines the so-called shading effect.

Now comparisons between the LES results obtained with the MGLET code and the experimental data from Kadota et al. (2007) are discussed. Fig. 7 compares the average streamlines and contours of the *u*-velocity component in the symmetry plane (top of the figure) and a wall-parallel plane (bottom of the figure) located near the mid-height of the cylinders ($y/D = 1.5$). Overall, there is fairly good correspondence between calculations and measurements,
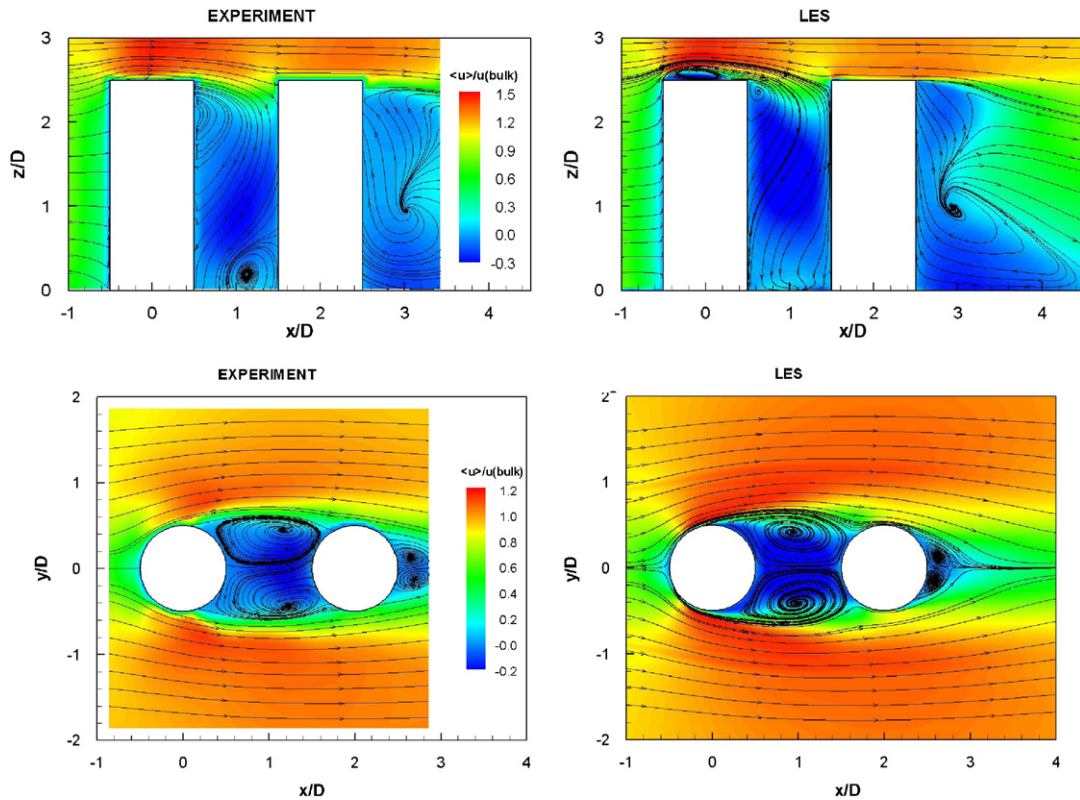
Fig. 7. Average streamlines in the centre plane (top) and near the mid-height of the cylinders (bottom). Left: experiment, right: Large Eddy Simulation results.

nevertheless some differences can be noticed. It was mentioned already that in the experiment no separation was detected on top of the first cylinder. Further, the experiments show a small recirculation region at the foot in front of the second cylinder which is absent in the LES. There is a tendency towards development of such a recirculation region, but there is no actual recirculation. The difference may be due to some differences in the approach-flow velocity as the development of the flow in this region is rather sensitive to this. The authors were only recently informed by the experimenters that the approach flow was not entirely uniform and had a thicker boundary layer than initially stipulated.

As can be seen from Fig. 7, the gap between the cylinders is entirely filled by the pair of recirculation zones, the size of which is in good agreement with the measurements, and there is a fairly strong downward flow almost everywhere in the gap, bringing in fluid from the top and moving it outwards around the second cylinder near the bottom. The flow behind the second cylinder is very different from the flow behind the first cylinder but also quite different from that behind a single cylinder. In the longitudinal centre plane there is a detached core of circulation just below the mid-height at which fluid rushes in from the sides to fill the wake at this height. There, the recirculation zones in the horizontal plane can be seen to be quite small (lower part of Fig. 7), much smaller than in the single-cylinder case. Above the core, an upward motion is caused behind the cylinder by the fairly high velocity of the attached flow over the top entraining fluid from below. Below mid-height there is an almost closed recirculation with the separation region in horizontal planes reaching further downstream, closer to what was observed behind the single cylinder. All this is in fairly good agreement with the experimental results, as can be seen from Fig. 7. A further comparison between measurements and simulation is presented in Fig. 8 in the form of velocity profiles at various x locations in the symmetry plane. As discussed above, the small recirculation on top of the first cylinder could not be captured by the PIV system leading to the discrepancy between measured and calculated velocities at $x/D = 0$. Deviations are also apparent for the velocity profile at $x/D = 1$ in the middle of the gap between the cylinders. Here, the negative velocity at mid-height is over-predicted and may be caused by the approach-flow velocity specified in the LES being somewhat different from the one in the experiment. It may also be partly caused by the assumption of a rigid lid which may not be fully justifiable in this
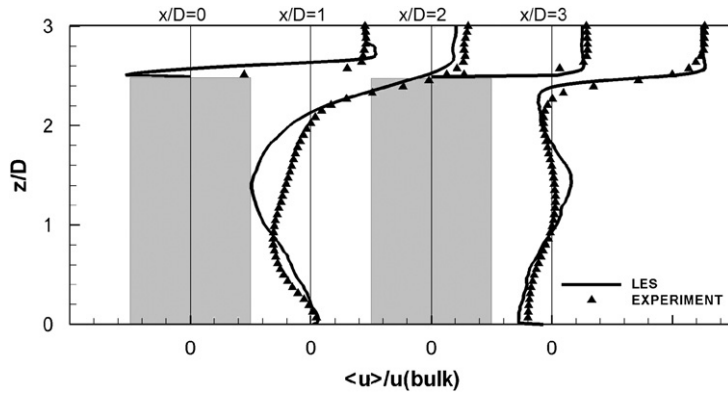
Fig. 8. Streamwise mean velocity in wall-normal direction at x/D equal to 0, 1, 2 and 3 (from left to right). –, LES; ▲, experiments of Kadota et al. (2007).
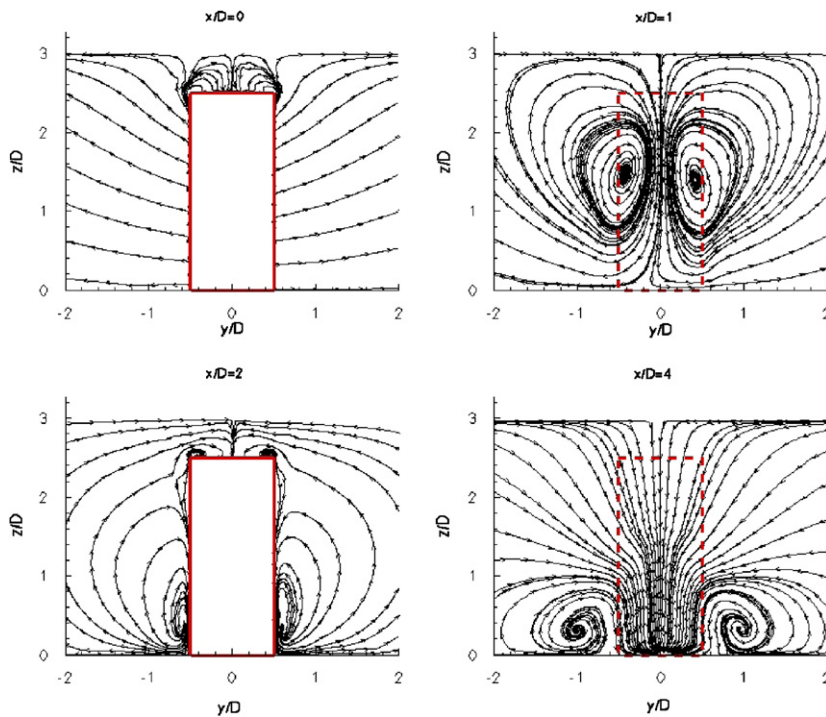

Fig. 9. Streamlines in planes normal to the x-axis at the middle of each cylinder, between them and downstream of the second one.

case where there is a fairly small distance between the top of the cylinders and the water surface causing non-negligible surface elevations over the cylinders, particularly the first one. The absence of recirculation on top of the second cylinder is evident from the vertical velocity distribution at $x/D = 2$, and the simulated and experimental distribution are in very good agreement. The complex flow behaviour behind the second cylinder can also be seen from the u-velocity profile in the symmetry plane at $x/D = 3$, where reasonable agreement between the calculations and the measurement is found. There is a reverse flow near the ground plate which turns into a positive flow near mid depth and turns again into a reverse flow near the free end of the cylinder.

Fig. 9 represents the secondary motion at various cross sections and allows us to follow the trailing vortices produced on the top of the upstream cylinder. In the first plane, located at the middle of the first cylinder, the formation of the two trailing vortices can be observed, similar to the structures obtained by smoke visualization by Roh and Park (2003).

These trailing vortices are moved downstream and downward by the mean motion, and in the middle of the gap between both cylinders their centres are located at $y/D \approx 1.5$ (similar values were obtained by Froehlich and Rodi (2004) for a single cylinder with the same ratio $H/D = 2.5$). These vortices then impinge on the second cylinder causing a secondary motion near the cylinder surface at a height of $y/D = 0.5$ and move further downward past this cylinder and merge with the HSV that is likely to be present there (see last plane at $x/D = 4$). On top of the second cylinder, two further very weak vortices are produced, but these decay quickly and are not visible in the planes downstream.

5. Conclusions

We have presented in this paper results of a Large Eddy Simulation of the flow around two cylinders arranged in tandem where one cylinder is located downstream of the other. The instantaneous and average flow reveals that the flow belongs to the reattachment regime; hence, as expected, no shedding vortices are formed in the gap between the cylinders.

The flow behaviour is different from a single cylinder flow because the second cylinder perturbs the formation of a von Karman vortex sheet and the trailing vortices formed on the top of the first cylinder.

Comparison with experimental data shows generally good agreement, although some differences are observed in the gap between the cylinders that could be due to some differences in the approach-flow velocity and the small submergence of the cylinders possibly causing changes in the water surface level above the upstream cylinder that was not taken into account in the LES.

Acknowledgements

References

Delery, J.M., 1992. Physics of vortical flows. Journal of Aircraft 29, 856–876.

Farrant, T., Tan, M., Price, W.G., 2000. A cell boundary element method applied to laminar vortex-shedding from arrays of cylinders in various arrangements. Journal of Fluids and Structures 14, 375–402.

Fischer-Antze, T., Stoesser, T., Bates, P.B., Olsen, N.R., 2001. 3D numerical modelling of open-channel flow with submerged vegetation. IAHR Journal of Hydraulic Research 39, 303–310.

Froehlich, J., Rodi, W., 2004. LES of the flow around a circular cylinder of finite height. International Journal of Heat and Fluid Flow 25, 537–548.

Germano, M., Piomelli, U., Moin, P., Cabot, W.T., 1991. A dynamic subgrid-scale eddy viscosity model. Physics of Fluids 3, 1760–1765.

Hain, R., Kaehler, Ch.J., Michaelis, D., 2007. Tomographic and time-resolved PIV measurements on a finite cylinder mounted on a flat plate. In: Proceedings of the 7th International Symposium on Particle Image Velocimetry, Rome, September 11–14.

Hunt, J.C.R., Wray, A.A., Moin, P., 1988. Eddies, stream, and convergence zones in turbulent flows. Center for Turbulence Research Report CTR-S88.

Igarashi, T., 1981. Characteristics of the flow around two circular cylinders arranged in tandem. Bulletin of JSME 24, 323–331.

Kadota, A., Aragao, R., Suzuki, K., 2007. Visualization of flow pattern around two-in-tandem cylinders. Personal communication.

Ljungkrona, L., Norberg, C.H., Sundén, B., 1991. Free-stream turbulence and tube spacing effects on surface pressure fluctuations for two tubes in an in-line arrangement. Journal of Fluids and Structures 5, 701–727.

Luo, S.C., Gan, T.L., Chew, T.S., 1987. Uniform flow past one (or two in tandem) finite length circular cylinder(s). Journal of Wind Engineering and Industrial Aerodynamics 59, 69–93.

Mittal, S., Kumar, V., Raghuvanshi, A., 1997. Unsteady incompressible flows past two cylinders in tandem and staggered arrangements. International Journal of Numerical Methods in Fluids 25, 1315–1344.

Oka, S., Kostic, Z.G., Sikmanovic, S., 1972. Investigation of the heat transfer process in tube banks in cross flow. In: International Seminar on Recent Development in Heat Exchangers, Trogir, Yugoslavia.

Papaioannou, G.V., Yue, D., Triantafyllou, M., Karniadakis, G., 2006. Three-dimensionality effects in flow around two tandem cylinders. Journal of Fluid Mechanics 558, 387–413.

Pattenden, R.J., Turnock, S.R., Zhang, X., 2005. Measurements of the flow over a low-aspect ratio cylinder mounted on a ground plate. Experiments in Fluids 39, 10–21.

Roh, S.C., Park, S.O., 2003. Vortical flow over the free end surface of a finite circular cylinder mounted on a flat plate. Experiments in Fluids 34, 63–67.

Stansby, P.K., Smith, P.A., Penoyre, R., 1987. Flow around multiple cylinders by the vortex method. In: Proceedings of the International Conference on Flow Induced Vibration, England, Cranfield, pp. 41–57.

Stone, H.L., 1968. Iterative solution of implicit approximation of multi-dimensional partial differential equations. SIAM Journal on Numerical Analysis 3.

Summer, D., Price, S.J., Païdoussis, M.P., 1999. Tandem cylinders in impulsively started flow. Journal of Fluids and Structures 13, 955–965.

Tanida, Y., Okajima, A., Watanabe, Y., 1973. Stability of a circular-cylinder oscillating in uniform flow or in a wake. Journal of Fluid Mechanics 61, 769–784.

Tremblay, F., Friedrich, R., 2001. An algorithm to treat flows bounded by arbitrarily shaped surfaces with Cartesian meshes. In: Notes on Numerical Fluid Mechanics. Springer, Berlin, p. 77.

Verzicco, R., Mohd-Yusof, J., Orlandi, P., Haworth, D., 2000. Large Eddy Simulation in complex geometric configurations using boundary body forces. AAIA Journal 38, 427–433.

Zdravkovich, M.M., 1987. The effect of interference between circular cylinders in cross flow. Journal of Fluids and Structures 1, 239–261.